

Valence subband structure of [100]-, [110]-, and [111]-grown GaAs-(Al,Ga)As quantum wells and the accuracy of the axial approximation

Z. Ikonić

Faculty of Electrical Engineering, University of Belgrade, Bulevar Revolucije 73, Belgrade, Serbia, Yugoslavia

V. Milanović

*Faculty of Electrical Engineering, University of Belgrade, Bulevar Revolucije 73, Belgrade, Serbia, Yugoslavia
and High Technical Post Telegraph and Telephone School, Zdravka Čelara 16, 11000 Belgrade, Serbia, Yugoslavia*

D. Tjapkin

*Faculty of Electrical Engineering, University of Belgrade, Bulevar Revolucije 73, Belgrade, Serbia, Yugoslavia
(Received 22 October 1991; revised manuscript received 20 April 1992)*

Block diagonalization of 4×4 Luttinger Hamiltonians, to be applied for hole-state quantization in [100]-, [110]-, and [111]-grown semiconductor quantum wells, is discussed and the accuracy of the axial approximation is analyzed.

Most work on semiconductor quantum wells (QW's) has been devoted to the [100] growth direction. Occasionally, however, other growth directions, specifically [110] and [111], are employed, resulting in remarkably different electronic structure in both the valence and conduction bands (e.g., Refs. 1–4). The valence-band structure is usually analyzed within the four-component envelope-function approximation, i.e., with heavy and light holes taken into account, and the split-off band neglected. Due to the double degeneracy of the resulting 4×4 Hamiltonian, it may be block diagonalized into two 2×2 blocks, which is particularly simple within the so-called axial approximation. In this paper we analyze the block diagonalization of 4×4 Hamiltonians to be applied in calculation of bound states in [100]-, [110], and [111]-grown QW's, and discuss the accuracy of the axial approximation.

Starting from the Luttinger 4×4 bulk Hamiltonian⁵ with $|j, m_j\rangle$ basis

$$H = (\gamma_1 + 5\gamma_2/2)k^2 I_4 - 2\gamma_2(k_x^2 J_x + k_y^2 J_y + k_z^2 J_z) - 4\gamma_3(k_x k_y J_{xy} + \text{c.p.}), \quad (1)$$

where $J_{ij} = (J_i J_j + J_j J_i)/2$, $i, j = x, y, z$ are the crystal cell axes, I_4 is the 4×4 unity matrix, J_i are the spin- $\frac{3}{2}$ matrices, $k^2 = k_x^2 + k_y^2 + k_z^2$, and $\gamma_{1,2,3}$ denote, here and throughout the paper, the Luttinger parameters with $\hbar^2/2m_0$ factors absorbed. Hamiltonians for various directions may readily be derived by expressing $J_{x,y,z}$ and $k_{x,y,z}$ in terms of their projections in the new coordinate systems, chosen so that one axis (e.g., new z , the quantization axis) is along the chosen direction, and the other two perpendicular to it. However, the exact forms of H (including the [100] case) depend on the phase convention adopted for $J_{x,y}$. If J_x is chosen to be imaginary and J_y real, the form used, e.g., in Refs. 6 and 7 for [100], Ref. 3 for [111], or Ref. 4 for all three directions, is obtained,

while real J_x and imaginary J_y lead to a slightly different, but otherwise equivalent form used, e.g., in Refs. 8–10. In this paper, we used the second option. Concerning cases other than [100], setting the new (rotated) x , y , and z axes along (1,0,-1), (0,1,0), and (1,0,1) directions of the initial system in the [110] case, and along (1,1,-2), (-1,1,0), and (1,1,1) in the [111] case, and, as conventional in this choice, ordering the states as $|\frac{3}{2}, \frac{3}{2}\rangle$, $|\frac{3}{2}, -\frac{1}{2}\rangle$, $|\frac{3}{2}, \frac{1}{2}\rangle$, and $|\frac{3}{2}, -\frac{3}{2}\rangle$, the 4×4 bulk Hamiltonians have the common form in all three cases, and read

$$H = \begin{pmatrix} T_+ & R & -S & 0 \\ R^\dagger & T_- & 0 & S \\ -S^\dagger & 0 & T_- & R \\ 0 & S^\dagger & R^\dagger & T_+ \end{pmatrix}, \quad (2)$$

where in the [100] case

$$\begin{aligned} T_\pm &= \gamma_1(k_x^2 + k_y^2 + k_z^2) \pm \gamma_2(k_x^2 + k_y^2 - 2k_z^2), \\ R &= (\sqrt{3}/2)[(\gamma_2 + \gamma_3)(k_x - ik_y)^2 \\ &\quad + (\gamma_2 - \gamma_3)(k_x + ik_y)^2], \\ S &= 2\sqrt{3}\gamma_3 k_z(k_x - ik_y), \end{aligned} \quad (3)$$

in the [110] case

$$\begin{aligned} T_\pm &= [2\gamma_1(k_x^2 + k_y^2) \mp \gamma_2 k_x^2 \pm 2\gamma_2 k_y^2 \pm 3\gamma_3 k_x^2 \\ &\quad + (2\gamma_1 \mp \gamma_2 \mp 3\gamma_3)k_z^2]/2, \\ R &= (\sqrt{3}/2)[-2\gamma_3(k_x - ik_y)^2 \\ &\quad + (\gamma_2 - \gamma_3)(2k_y^2 - k_x^2 - k_z^2)], \\ S &= 2\sqrt{3}[\gamma_3(k_x - ik_y) + (\gamma_2 - \gamma_3)k_x]k_z, \end{aligned} \quad (4)$$

and in the [111] case

$$\begin{aligned}
T_{\pm} &= (\gamma_1 \pm \gamma_3)(k_x^2 + k_y^2) + (\gamma_1 \mp 2\gamma_3)k_z^2, \\
R &= -2[(\gamma_2 + 2\gamma_3)/\sqrt{3}](k_x - ik_y)^2 \\
&\quad + 4[(\gamma_2 - \gamma_3)/\sqrt{6}](k_x + ik_y)k_z, \\
S &= 2[(2\gamma_2 + \gamma_3)/\sqrt{3}](k_x - ik_y)k_z \\
&\quad - 2[(\gamma_2 - \gamma_3)/\sqrt{6}](k_x + ik_y)^2.
\end{aligned} \tag{5}$$

They have slightly different forms from those of Ref. 4 due to different phase conventions for the $J_{x,y}$ we adopted. It is also of interest, when finding states in asymptotically flat confining potentials, to give the $k_z(E, k_x, k_y)$ dispersion in these cases. The secular equation $H\Psi = E\Psi$ in the [100] and [110] cases gives a biquadratic fourth-order polynomial in k_z^2 , with solutions

$$k_z^2 = (a \pm \sqrt{b})/c, \tag{6}$$

where in the [100] case

$$\begin{aligned}
a &= \gamma_1 E - (k_x^2 + k_y^2)(\gamma_1^2 + 2\gamma_2^2 - 6\gamma_3^2), \\
b &= 4[\gamma_2^2 E^2 - 3E(k_x^2 + k_y^2)\gamma_1(\gamma_2^2 - \gamma_3^2) \\
&\quad + 3(k_x^4 + k_y^4)(\gamma_1^2\gamma_2^2 - \gamma_1^2\gamma_3^2 - 2\gamma_2^2\gamma_3^2 - \gamma_2^4 + 3\gamma_3^4) \\
&\quad + 3k_x^2 k_y^2(\gamma_1^2\gamma_2^2 - \gamma_1^2\gamma_3^2 - 8\gamma_2^2\gamma_3^2 + 2\gamma_2^4 + 6\gamma_3^4)], \\
c &= \gamma_1^2 - 4\gamma_2^2
\end{aligned} \tag{7}$$

and in the [110] case

$$\begin{aligned}
a &= -\gamma_1 E + k_x^2(\gamma_1^2 - 7\gamma_2^2 + 3\gamma_3^2) + k_y^2(\gamma_1^2 + 2\gamma_2^2 - 6\gamma_3^2), \\
b &= E^2(\gamma_2^2 + \gamma_3^2) + 6E\gamma_1(\gamma_2^2 - \gamma_3^2)(2k_x^2 - k_y^2) \\
&\quad - 12k_x^4(\gamma_1^2\gamma_2^2 - \gamma_1^2\gamma_3^2 + 4\gamma_2^2\gamma_3^2 - 4\gamma_2^4) \\
&\quad + 9k_y^4(\gamma_1^2\gamma_2^2 - \gamma_1^2\gamma_3^2 - 4\gamma_2^2\gamma_3^2 + 4\gamma_3^4) \\
&\quad - 12k_x^2 k_y^2(\gamma_1^2\gamma_2^2 - \gamma_1^2\gamma_3^2 - 8\gamma_2^2\gamma_3^2 + 2\gamma_2^4 + 6\gamma_3^4), \\
c &= -\gamma_1^2 + \gamma_2^2 + 3\gamma_3^2.
\end{aligned} \tag{8}$$

In the [111] case, however, the secular equation gives an eight-order polynomial, with odd powers of k_z present as well, but it may be recast as a square of a fourth-order polynomial

$$\begin{aligned}
&[-\gamma_1^2 + 4\gamma_3^2]k_z^4 + 2[E\gamma_1 - (k_x^2 + k_y^2)(\gamma_1^2 - 4\gamma_2^2)]k_z^2 \\
&\quad + [8k_x(k_x^2 + k_y^2)(\gamma_3^2 - \gamma_2^2)/\sqrt{2}]k_z \\
&\quad + [-E^2 + 2E\gamma_1(k_x^2 + k_y^2) \\
&\quad \quad - (\gamma_1^2 - \gamma_2^2 - 3\gamma_3^2)(k_x^2 + k_y^2)^2] = 0.
\end{aligned} \tag{9}$$

For nonzero k_x and k_y , it is not biquadratic; hence its solutions are not of the $\pm k_z$ type, unlike those in [100] and [110] cases. Eigenvectors of the above Hamiltonians are analogous to those in Ref. 6.

To make the envelope function Hamiltonians from Eqs. (2)–(5), where in principle the γ 's depend on z , one makes the usual substitution $\{\gamma\}k_z \rightarrow (-i/2)[\{\gamma\}(d/dz) + (d/dz)\{\gamma\}]$ and $\{\gamma\}k_z^2 \rightarrow$

$-(d/dz)\{\gamma\}(d/dz)$, where the symbol $\{\gamma\}$ denotes that particular combination of $\gamma_{1,2,3}$ that stands by k_z or k_z^2 . The boundary conditions at interfaces are easily written following the prescription of Ref. 11: writing the Hamiltonian matrix as $H = A d^2/dz^2 + B d/dz + C$, the components of the state vector $\Psi[f_1, f_2, f_3, f_4]^T$ and $[A d/dz + B/2]\Psi$ are continuous across the interfaces (f_1, f_2, f_3 , and f_4 are the z -dependent amplitudes of the above spin states). The procedure for finding bound states is described in Ref. 6. The Hamiltonian (2) may be block diagonalized by a unitary transform matrix U (Refs. 8 and 12)

$$U = (1/\sqrt{2}) \begin{pmatrix} e^{-i\phi} & 0 & 0 & -e^{i\phi} \\ 0 & e^{-i\eta} & -e^{i\eta} & 0 \\ 0 & e^{-i\eta} & e^{i\eta} & 0 \\ e^{-i\phi} & 0 & 0 & e^{i\phi} \end{pmatrix}, \tag{10}$$

where ϕ and η are chosen so that $H' = UH U^\dagger$ is block diagonal, the new set of states being given as $[F_1, F_2, F_3, F_4]^T = U[f_1, f_2, f_3, f_4]^T$. The block diagonalization is in the literature usually used together with the axial approximation ($\gamma_2 = \gamma_3$ in off-diagonal terms), but in fact there is no relation between the two, and the choice

$$e^{i4\phi} = -(RS)/(R^\dagger S^\dagger), \quad e^{i2\eta} = -(S/S^\dagger)e^{-i2\phi}, \tag{11}$$

leads to block diagonalization of H , whatever values γ_2 and γ_3 may have. However, ϕ and η now depend on γ_2 and γ_3 , as well as on k_x and k_y . Within the axial approximation the difference between γ_2 and γ_3 is neglected, and Eq. (11) reduces to the familiar result $\phi = 3\pi/4 - 3\theta/2$, $\eta = -\pi/4 + \theta/2$, and $\theta = \arctan(k_y/k_x)$, independent on $\gamma_{2,3}$. Applying this unitary transform to (2), we find that in the [100] and [111] cases blocks of the new Hamiltonians H' depend on $k_i^2 = k_x^2 + k_y^2$ only, making them axially symmetric. In the [110] case, however, the diagonal terms of H' have different coefficients multiplying k_x^2 and k_y^2 , unless $\gamma_2 = \gamma_3$. If the axially symmetric Hamiltonian is to be obtained, diagonal terms have to be modified, e.g., by taking the average of coefficients standing by k_x^2 and k_y^2 as the multiplier of k_i^2 . Thus, there is no strictly axial approximation, as distinct from the spherical approximation in the [110] case. Now all the three Hamiltonians may be conveniently written in the common form, with the upper 2×2 block reading

TABLE I. Γ coefficients of the Hamiltonian (12) for [100], [110], and [111] orientations.

	[100]	[110]	[111]
$\Gamma_{i\pm}$	$\gamma_1 \pm \gamma_2$	$(4\gamma_1 \pm \gamma_2 \pm 3\gamma_3)/4$	$\gamma_1 \pm \gamma_3$
$\Gamma_{z\pm}$	$\gamma_1 \mp 2\gamma_2$	$(2\gamma_1 \mp \gamma_2 \mp 3\gamma_3)/2$	$\gamma_1 \mp 2\gamma_3$
Γ_r	$\sqrt{3}(\gamma_2 + \gamma_3)/2$	$\sqrt{3}\gamma_3$	$(\gamma_2 + 2\gamma_3)/\sqrt{3}$
Γ_i	$2\sqrt{3}\gamma_3$	$2\sqrt{3}\gamma_3$	$2(2\gamma_2 + \gamma_3)/\sqrt{3}$

$$H_U = \begin{bmatrix} X_+ & Y \\ Y^\dagger & X_- \end{bmatrix}$$

$$X_\pm = \Gamma_{t\pm} k_t^2 + \Gamma_{z\pm} k_z^2, \quad (12)$$

$$Y = \Gamma_r k_t^2 - i\Gamma_i k_t k_z,$$

$$a = E(\Gamma_{z+} + \Gamma_{z-}) + k_t^2(\Gamma_i^2 - \Gamma_{t+}\Gamma_{z-} - \Gamma_{t-}\Gamma_{z+}),$$

$$b = E^2(\Gamma_{z+} - \Gamma_{z-})^2 + 2Ek_t^2(\Gamma_i^2\Gamma_{z-} + \Gamma_i^2\Gamma_{z+} - \Gamma_{t+}\Gamma_{z-}^2 + \Gamma_{t+}\Gamma_{z-}\Gamma_{z+} + \Gamma_{t-}\Gamma_{z-}\Gamma_{z+} - \Gamma_{t-}\Gamma_{z+}^2) \\ + k_t^4(\Gamma_i^4 - 2\Gamma_i^2\Gamma_{t+}\Gamma_{z-} - 2\Gamma_i^2\Gamma_{t-}\Gamma_{z+} + 4\Gamma_i^2\Gamma_{z-}\Gamma_{z+} + \Gamma_{t+}^2\Gamma_{z-}^2 - 2\Gamma_{t+}\Gamma_{t-}\Gamma_{z+}\Gamma_{z-} + \Gamma_{t-}^2\Gamma_{z+}^2), \quad (13)$$

$$c = 2\Gamma_{z+}\Gamma_{z-}.$$

Boundary conditions at the interface are the continuity of wave function components, and of

$$\begin{bmatrix} \Gamma_{z+} d/dz & \Gamma_i k_t/2 \\ \Gamma_i k_t/2 & -\Gamma_{z-} d/dz \end{bmatrix} \begin{bmatrix} F_1 \\ F_2 \end{bmatrix}. \quad (14)$$

To test the accuracy of the axial approximation in the three cases, we made numerical calculations for GaAs QW's embedded in $\text{Al}_{0.3}\text{Ga}_{0.7}\text{As}$ bulk. Luttinger parameters are taken as $\gamma_1=6.85$ (3.45), $\gamma_2=2.10$ (0.68), and $\gamma_3=2.90$ (1.29) for GaAs (AlAs), and are linearly interpolated for the alloy. Barrier height at the interface is $U_0=150$ meV. The dispersion for the first three bound

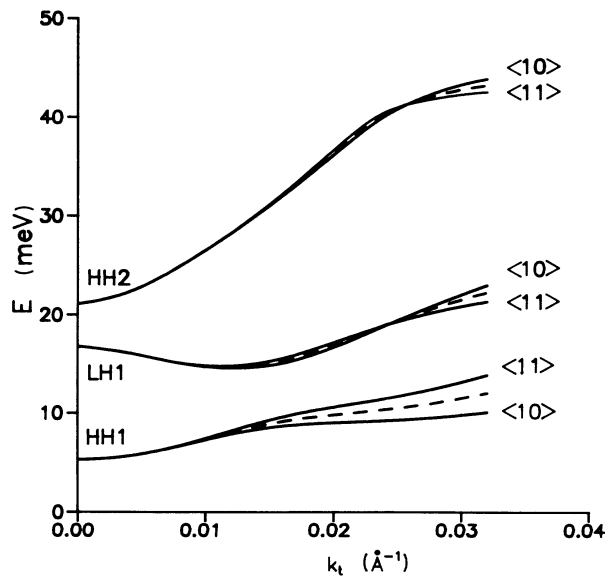


FIG. 1. Dispersion of the first three bound states of a $d = 120$ Å wide GaAs QW in $\text{Al}_{0.3}\text{Ga}_{0.7}\text{As}$ bulk, grown in the [100] direction. Full lines correspond to the exact calculations, with k_t along k_x ($\langle 10 \rangle$), or midway between k_x and k_y ($\langle 11 \rangle$), and broken lines to the axial approximation results.

and the lower one having analogous form. The expressions for Γ coefficients are given in Table I.

The $k_z(E, k_t)$ dispersion are again given by Eq. (6) in all three cases (solutions are now of the $\pm k_z$ type for [111] as well), where

states in $d = 120$ Å wide QW's grown in the [100], [110], and [111] directions is given in Figs. 1–3. The errors introduced by the axial approximation are larger for lower levels and for larger k_t . While the errors in the [100] and [111] cases may be considered as acceptable, those in the [110] case are rather large. Calculations for thinner wells show that all these errors tend to decrease, but, for the [110] QW's, remain high enough to rule out the use of the axial approximation in reasonably accurate calculations, as has also been found in Ref. 4. This high error may be ascribed to the fact that this case is not distinct from the spherical approximation, which is known to give larger errors than the axial approximation in the [100] case as well. In Fig. 4 we give the level's angular dispersion (with k_t fixed, but its orientation varies), together with the nondispersive results of the axial approximation. Oscillations with periods reflecting the structure symmetry

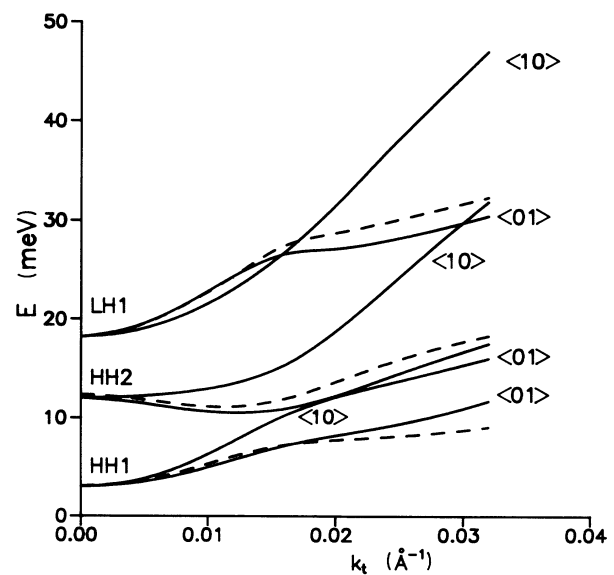


FIG. 2. Same as Fig. 1, but for the [110] growth, and k_t is along k_x ($\langle 10 \rangle$) or k_y ($\langle 01 \rangle$). The relation between the new (x, y, z) axes and the unit-cell cube axes is given in the text.

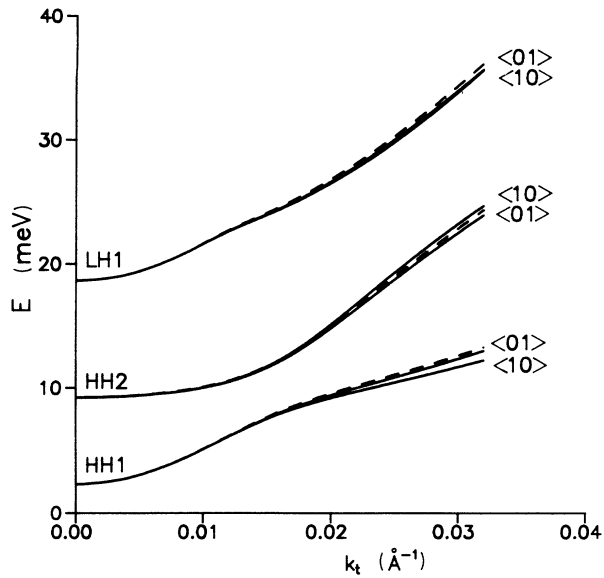


FIG. 3. Same as in Fig. 2, but for the [111] growth.

for the corresponding growth directions are clearly visible.

In conclusion, the accuracy of the axial approximation is best in [111]-grown, slightly less so in [100]-grown QW's, but is quite low in the [110]-grown case, for which the exact Hamiltonian (2) and (4) should be used instead,

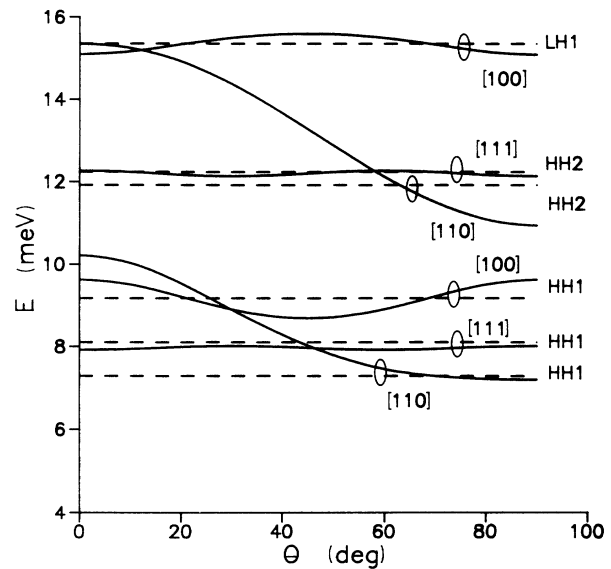


FIG. 4. The angular dispersion for the lowest two bound states of [100]-, [110]-, and [111]-grown QW's, with parameters given in Fig. 1. The magnitude of k_t is fixed at 0.016 \AA^{-1} , and its direction angle varies, $\theta = \arctan(k_y/k_x)$.

possibly with block diagonalization (10)–(11).

The authors would like to express their thanks to Dr. E. P. O'Reilly and Dr. A. Ghiti (University of Surrey, U.K.) for very helpful discussions.

¹L. W. Molenkamp *et al.*, Phys. Rev. B **38**, 4314 (1988).

²G. P. Srivastava, R. J. Gordon, and Z. Ikončić, Superlatt. Microstruct. **9**, 43 (1991).

³W. Batty, U. Ekenberg, A. Ghiti, and E. P. O'Reilly, Semicond. Sci. Technol. **4**, 904 (1989).

⁴G. E. W. Bauer, in *Spectroscopy of Semiconductor Microstructures*, edited by G. Fasol, A. Fasolino, and P. Lugli (Plenum, New York, 1989), p. 381.

⁵J. M. Luttinger, Phys. Rev. **102**, 1030 (1956).

⁶L. C. Andreani, A. Pasquarello, and F. Bassani, Phys. Rev. B **36**, 5887 (1987).

⁷M. Altarelli, U. Ekenberg, and A. Fasolino, Phys. Rev. B **32**, 5138 (1985).

⁸A. Twardowski and C. Hermann, Phys. Rev. B **35**, 8144 (1987).

⁹D. Ahn, S. L. Chuang, and Y-C. Chang, J. Appl. Phys. **64**, 4056 (1988).

¹⁰D. Ahn and S. L. Chuang, IEEE J. Quantum Electron. **26**, 13 (1990).

¹¹R. Eppenga and M. F. H. Schuurmans, Phys. Rev. B **37**, 10 923 (1987).

¹²D. A. Broido and L. J. Sham, Phys. Rev. B **31**, 888 (1985).